Transmission and Unvaccinated-Only Testing in Populations of Mixed Vaccination Status

Kate M. Bubar*[1], Casey E. Middleton*[2], Kristen K. Bjorkman[3], Roy Parker[4,3,5], and Daniel B. Larremore[2,3]

[1]*Department of Applied Mathematics, University of Colorado Boulder*
[2]*Department of Computer Science, University of Colorado Boulder*
[3]*BioFrontiers Institute, University of Colorado Boulder*
[4]*Department of Biochemistry, University of Colorado Boulder*
[5]*Howard Hughes Medical Institute*

Abstract

In populations with mixed vaccination status, testing programs focused on the unvaccinated have been proposed and enacted to mitigate the spread of SARS-CoV-2. While the benefits of universal SARS-CoV-2 screening are well established, it is unclear how the benefits of unvaccinated-only testing depend on population vaccination rate. Here, we introduce and analyze a model of SARS-CoV-2 transmission in which a variable fraction of the population is fully vaccinated and those who remain unvaccinated are proactively tested for infection, while varying transmission rates, vaccine performance parameters, and the degree of social mixing between vaccinated and unvaccinated populations. We find that unvaccinated testing programs are effective only when compliance is high and testing is frequent, and when vaccine coverage is low or moderate. However, in highly vaccinated populations, the impact of testing unvaccinated individuals decreases, and, by analyzing the possible modes of transmission within and between the unvaccinated and vaccinated populations, we show that the unvaccinated community ceases to be the dominant driver of transmission. By evaluating a wide range of scenarios, this work focuses on elucidating general principles, finding broadly that resources devoted to routine testing of the unvaccinated population could be reallocated to other needs when vaccine coverage is sufficiently high.

* C.E.M. and K.M.B. contributed equally to this work.
To whom correspondence should be addressed: daniel.larremore@colorado.edu

Introduction

SARS-CoV-2 has created a world-wide pandemic that is beginning to be countered in some areas by widespread vaccination. COVID-19 vaccines are not only extremely effective at preventing severe disease (vaccine efficacy, VE $> 90\%$, [1]), but they also decrease susceptibility to infection ($\text{VE}_S = 74\%$ Pfizer-BioNTech; 85% Moderna [2]) and further decrease rates of onward transmission ($\text{VE}_I = 62\%$ [2]). In spite of these reductions, so-called vaccine breakthrough infections and subsequent transmission have been widely documented [3], raising the question of how to further mitigate transmission in partially vaccinated populations.

Prior to the approval of COVID-19 vaccines, transmission mitigation via consistent population testing was shown to be an effective approach to break chains of transmission and decrease the burden of COVID-19 using both RT-PCR [4–6] and rapid antigen testing [6, 7]. Specifically, testing is effective at the community level because it decreases transmission *from* individuals who are already infected [6, 8]. However, this means that the impact of testing focused only on the unvaccinated population, as has been proposed [9–11], may be limited by the extent to which transmission is driven by the unvaccinated population.

In this study, we model the spread of SARS-CoV-2 in populations of mixed vaccination status, focusing on two critical questions. First, how do vaccinated and unvaccinated populations each contribute to community spread, and how do those contributions vary with vaccination rates? Second, how do testing programs focused on unvaccinated individuals alone affect community spread? Our study's goals are not to make perfectly calibrated predictions, but instead to elucidate more general principles of unvaccinated-only testing in a partially vaccinated population, and, as such, our analyses consider a wide range of parameters and scenarios.

Results

Vaccination rates affect the dominant mode of transmission

To examine the dynamics of transmission in a population with mixed vaccination status, we first modeled transmission within and between communities of vaccinated (v) and unvaccinated (u) individuals in the absence of a testing program. Based on a standard Susceptible Exposed Infected Recovered (SEIR) model, we explicitly tracked the four transmission modes by which an infection might spread: $u \to u$, $u \to v$, $v \to u$, and $v \to v$ (Fig. 1a; see Materials and Methods). To model a population open to movement, all susceptible individuals were subject to a small, constant rate of exposure, with vaccinated individuals partially protected against subsequent infection. Because precise estimates of the basic reproductive number R_0 vary by context and over time, our analyses consider values inclusive of possible non-pharmaceutical interventions like masking and social distancing, and thus range from 2 to 6.

In a modeled population with 55% vaccination rate (corresponding to U.S. estimates as of Sept. 22, 2021 [12]), outbreaks still occurred, despite assuming a partially mitigated delta variant ($R_0 = 4$) and vaccines with 80% effectiveness in blocking infection ($\text{VE}_S = 0.80$ [2]) and a further 62% effectiveness in blocking onward transmission upon infection ($\text{VE}_I = 0.62$ [2]). During the ensuing outbreak, we found that 63% of total infections occurred in unvaccinated individuals, despite making up only 45% of the population (Fig. 1c), with the remaining 37% occurring among the vaccinated (so-called breakthrough infections). Furthermore, the peak burden of disease occurred first in the unvaccinated community and then one week later in the vaccinated community (Fig. 1b), a known consequence of disease dynamics in populations with

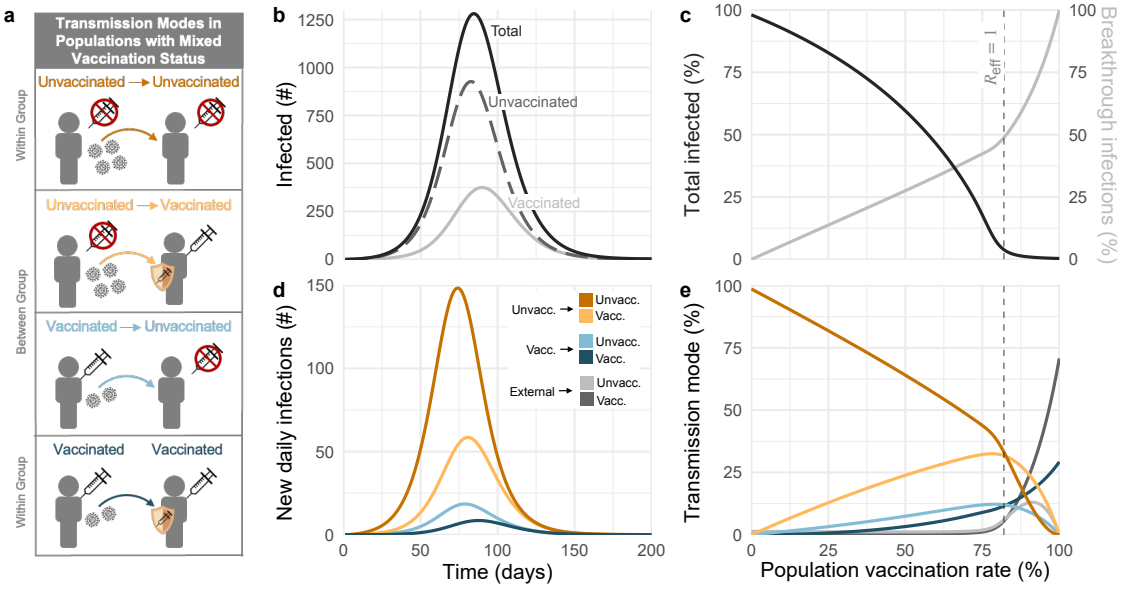

Figure 1: **Vaccination affects which populations drive transmission.** (a) Diagram of four transmission modes within and between vaccinated and unvaccinated communities, where vaccines protect against both infection and transmission. (b) Total infections over time (solid black), stratified by unvaccinated (dashed gray) and vaccinated (solid gray) populations, with a 55% vaccination rate. (c) Cumulative infections as a percentage of population (black) and of total infections occurring among the vaccinated (gray) for varying vaccination rates. (d) Daily transmission events separated and colored by transmission mode (see legend; 55% vaccination rate). External infections (not shown) persist at a daily level below 1. (e) Transmission mode as a percentage of total infections (see legend) for varying vaccination rates. Vertical dashed lines denote the vaccination rate at which $R_{\text{eff}} = 1$. $R_0 = 4$ for all plots, and dynamics are shown in the absence of testing.

heterogeneous susceptibility and transmissibility [13, 14]. By examining the four modes of transmission separately, we observe that infections in both communities were driven predominantly and consistently by the unvaccinated community ($u \to u$, $u \to v$). These differences occurred despite a "well mixed" modeling assumption—namely, that neither type of individual is more or less likely to associate with a member of their own group vs the other group.

Vaccination rates vary widely across the U.S. [12] and the world [15] due to impacts of both vaccine availability [15] and refusal [16]. We therefore asked how a population's vaccination rate would affect our observations about total infections, breakthrough infections, and the relative impacts of the four modes of transmission. This analysis revealed three important points.

First, our results reinforce the fact that increased levels of vaccination markedly reduce total infections, even before the so-called "herd immunity" threshold where the effective reproductive number $R_{\text{eff}} = 1$ (Fig. 1c; dashed line). Herd immunity in a well-mixed population is achieved when the vaccination rate ϕ satisfies

$$\phi \geq \frac{1 - 1/R_0}{1 - (1 - \text{VE}_S)(1 - \text{VE}_I)}, \tag{1}$$

after which transmission is no longer self-sustaining even in the absence of testing. In our model, this occurs

Proportion of population vaccinated (%) when cumulative transmission is no longer dominated by unvaccinated							
		well mixed			homophily		
R_0		2	4	6	2	4	6
Testing	no testing	74	87	91	82	90	93
	weekly testing, 50% compliance	66	83	88	76	87	91
	weekly testing, 99% compliance	51	75	83	65	82	87
	2× weekly testing, 99% compliance	0	33	55	0	49	67

Table 1: **Vaccination rate at which the dominant mode of transmission shifts.** R_0 values of 2, 4, and 6 are considered under well mixed ($q = 0$) and homphilic ($q = 0.8$) mixing assumptions. $\text{VE}_S = 80\%, \text{VE}_I = 62\%$.

at vaccination rates of 54%, 81%, and 90% for $R_0 = 2$, 4, and 6, respectively.

Second, as vaccination rates increased, the fraction of the declining infections classified as vaccine breakthroughs increased monotonically but nonlinearly (Fig. 1c). These observations held true for alternative assumptions about transmission-blocking vaccine effectiveness (Supplementary Fig. S1). Thus, our results set the expectation that with increasing vaccination rates there will be decreasing overall infections but a higher proportion of breakthrough infections.

Third, at a certain level of vaccination, the unvaccinated community ceased to be the primary driver of transmission. Under our baseline modeling conditions ($R_0 = 4$, $\text{VE}_S = 0.8$, $\text{VE}_I = 0.62$), this transition occurred when 87% or more of the population was vaccinated (Fig. 1e). The exact point of this shift away from unvaccinated-driven transmission varied under alternative assumptions about R_0 (Table 1) and transmission-blocking vaccine effectiveness (Tables S2 and S3), but always fell between 74% ($R_0 = 2$) and 91% ($R_0 = 6$) vaccine coverage in the absence of testing. Interestingly, for vaccines with strong transmission-blocking effects ($\text{VE}_I = 0.62$), the transition away from unvaccinated-driven transmission occurred after the herd immunity threshold, but prior to the herd-immunity threshold when weaker transmission-blocking effects were assumed ($\text{VE}_I = 0.3$ or 0). Thus, while COVID-19 morbidity and mortality are likely to remain concentrated primarily in unvaccinated populations, only a minority of infections will occur in—and will be driven by—the unvaccinated community when vaccine coverage is sufficiently high.

Unvaccinated-only testing is of limited value in highly vaccinated populations

To explore the impact of unvaccinated-only testing on population transmission, we modified our simulations so that a positive test would result in an unvaccinated individual isolating to avoid infecting others [17]. We considered test sensitivity equivalent to RT-PCR with a one-day delay between sample collection and diagnosis under three testing paradigms: twice-weekly testing with 99% compliance, weekly testing with 99% compliance, and weekly testing with 50% compliance—a value which reflects observed compliance with a weekly testing mandate in the absence of strong incentives or penalties [4].

Our simulations show that unvaccinated-only testing decreases total infections regardless of testing program and vaccination rate (Fig. 2). As expected, testing programs with higher frequency and compliance outperform those with lower frequency or compliance [6]. By reducing transmission from unvaccinated individuals, these programs also reduce $u \to u$ and $u \to v$ transmission modes, shifting the cutoff values at

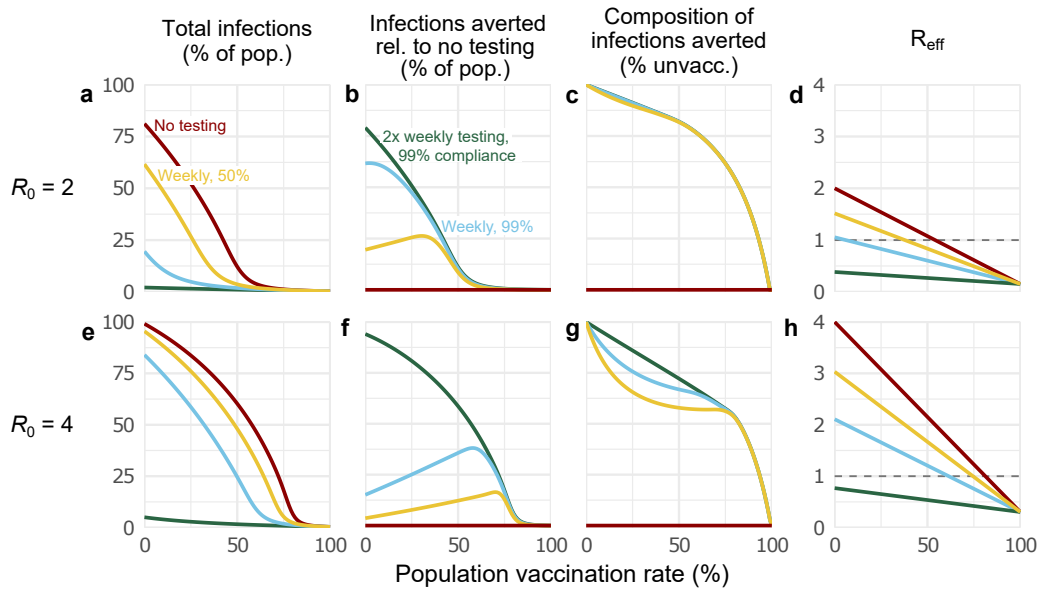

Figure 2: **Impact of unvaccinated-only testing on transmission.** Results are shown for varying vaccination rates under four testing regimens: no testing (red), weekly testing with 50% compliance (yellow), weekly testing with 99% compliance (blue), and twice-weekly testing with 99% compliance (green). (a and e) Percentage of population infected and (b and f) percentage of infections averted due to testing relative to no testing over population vaccination rate. (c and g) Percentage of total infections averted in the unvaccinated community out of the total number of infections averted. (d and h) Effective reproductive number R_{eff} over population vaccination rate. The gray dashed line indicates where $R_{\text{eff}} = 1$. For all simulations, $\text{VE}_S = 0.80$ and $\text{VE}_I = 0.62$. Top row $R_0 = 2$. Bottom row $R_0 = 4$.

which cumulative transmission is no longer dominated by the unvaccinated community to lower vaccination rates (Table 1 and Supplementary Tables S2 and S3).

As vaccination rates rise, the overall burden of disease decreases, meaning that, in absolute terms, testing programs avert fewer and fewer infections (Fig. 2a,e) until and beyond the herd immunity threshold given by Eq. (1). However, in relative terms, testing programs avert a larger proportion of infections (Fig. 2b,f and Supplementary Fig. S2), up until a particular vaccination rate is achieved. When vaccination rates exceed this value, both the absolute and relative numbers of infections avoided by testing drop rapidly, an observation which echoes model-based analysis of proactive testing of the unvaccinated and vaccinated alike [8]. For example, our analyses show that unvaccinated-only testing has the greatest impact on total infections when less than 54% of the population is vaccinated for low transmission scenarios ($R_0 = 2$; Fig. 2b) or when less than 81% of the population is vaccinated for high transmission scenarios ($R_0 = 4$; Fig. 2f). In short, our analyses show that testing the unvaccinated population to mitigate transmission is effective only when R_{eff} of the entire community is greater than 1.

In contrast, the maximum number of infections averted by testing occurs, for any program, at or around the point where testing decreases R_{eff} to 1 (Fig. 2, Supplementary Fig. S2). This occurs at vaccination rate

$$\phi = \frac{1 - \theta - 1/R_0}{1 - \theta - (1 - \text{VE}_S)(1 - \text{VE}_I)}, \tag{2}$$

and is driven lower as θ, the fraction by which testing curtails transmission by the unvaccinated, increases. This observation reinforces the fact that when testing tips the system from a regime with intrinsic growth ($R_{\text{eff}} > 1$) to a regime with intrinsic decline ($R_{\text{eff}} < 1$), its impacts are maximized. As such, for vaccination levels beyond this rate—and particularly when $R_{\text{eff}} < 1$ due to vaccination alone—testing-driven reductions in infections are markedly diminished (Fig. S2). This argues that continued testing for SARS-CoV-2 among the unvaccinated will be of limited value as vaccination rates become sufficiently high (see Discussion).

In regimes where unvaccinated-only testing had an observable impact on limiting SARS-CoV-2 infections, infections were predominantly averted in the unvaccinated population (Fig. 2c,g). These observations held true for all testing programs and transmission rates except for when $R_0 = 6$ (Fig. S2), representing unmitigated spread of a delta-like variant in a population with no prior immunity. Thus, we find that testing of the unvaccinated, when impactful, preferentially protects the unvaccinated population.

Homophily in contact patterns by vaccination status alters transmission modes and the impact of testing

Social ties may be correlated with vaccination status, such that those who are vaccinated or unvaccinated tend to associate with others of the same status more than one would expect from their population sizes alone. Because this type of social homophily would impact the proportions of the four inter- and intra-group transmission modes, we explored its effect by introducing a tunable homophily parameter into our model, increasing contacts between people with the same vaccination status while decreasing vaccination-discordant contacts. This approach preserves each group's total contact rate, regardless of the strength of homophily, by adjustably "rewiring" inter-group contacts into intra-group contacts (see Materials and Methods).

In the absence of testing, we observed that homophily shifted modes of transmission by increasing the dominance of the $u \to u$ transmission mode, while leaving the $v \to v$ mode unchanged (Fig. 3a, b). In contrast, infections transmitted $v \to u$ were markedly reduced, while those transmitted $u \to v$ were somewhat reduced for vaccination rates under 80-85%. Across values of R_0, homophily increased the range of vaccination rates for which the unvaccinated community drove a majority of transmission (Table 1 and Supplementary Fig. S3).

On its face, homophily's intensification of transmission within the unvaccinated community—a group targeted by unvaccinated testing programs—might lead one to hypothesize that homophily would increase the impact of targeted testing. However, we observe that the opposite is true, with typically fewer infections averted through testing when homophily is present. This is due to the fact that, in addition to altering transmission modes, homophily tends to increase R_{eff} (Fig. 3). In turn, this upward shift in R_{eff} increases the vaccination rates at which testing's effects are maximized ($R_{\text{eff}} = 1$ inclusive of testing) and similarly increases the subsequent vaccination rates at which testing's effects diminish rapidly ($R_{\text{eff}} = 1$ without testing). Although closed-form equations for these key vaccination rates, as in Eqs. (1) and (2), are not possible with homophily, the relationship between vaccination rate and R_{eff} is straightforward to calculate (Fig. 3e). Finally, in the regimes where unvaccinated-only testing had a substantial impact, the majority of averted infections were averted from unvaccinated individuals, regardless of homophily (Figs. 3 and S3).

In short, homophily shifts modes of transmission into the unvaccinated community and increases R_{eff}. This pushes the levels of vaccination required for three key transition points higher by 5-10%: (i) the point where the unvaccinated community no longer drives a majority of transmission (Tables 1, S2, and S3),

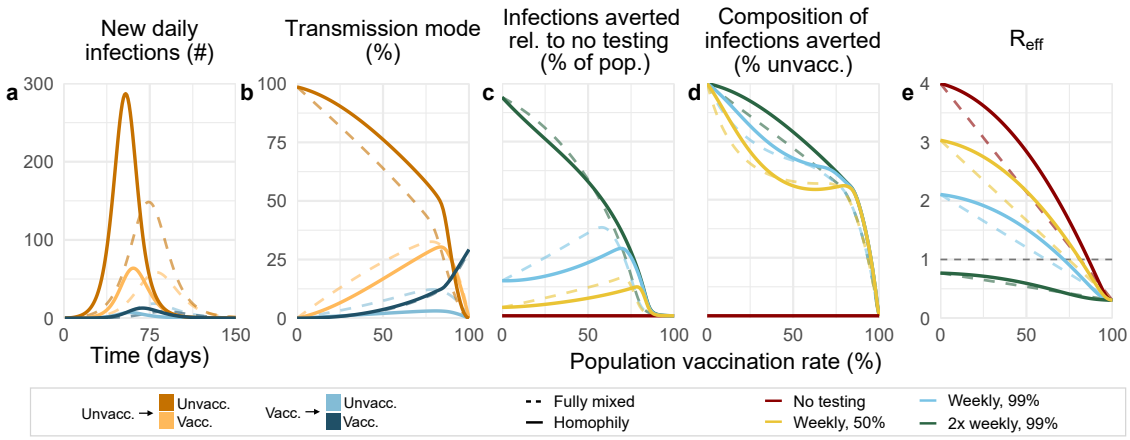

Figure 3: **Homophily affects transmission modes and impact of testing.** Panels contrast well-mixed contact patterns (no homophily; dashed lines) with homophilic contact patterns (solid lines) over population vaccination rates. (a) Homophily shifts the four modes of transmission, and in particular leads to increased $u \to u$ transmission. (b) Homophily increases $u \to u$ transmission across vaccination rates and (c) has mixed effects on the number of infections averted due to testing. (d) Homophily alters the composition of the infections averted by testing in both directions, as indicated by arrows. (e) Homophily increases the effective reproductive value (R_{eff}) non-linearly, except in instances where $R_{\text{eff}} < 1$ in the absence of homophily. $R_0 = 4$ in all plots.

(ii) the point where the impact of testing is maximized (Fig. 3c,e), and (iii) the point at which all testing programs cease to have a substantial impact (Fig. 3c,e).

Discussion

In this analysis, we find that in communities with mixed vaccination status, routine SARS-CoV-2 testing programs focused on the unvaccinated community can reduce infection, but in a manner dependent on two conditions. First, effective screening testing requires high participation to be most impactful, reinforcing the need for mechanisms to encourage or enforce high participation. Second when vaccination rates are high enough to curtail transmission on their own, testing the remaining unvaccinated population averts few infections in both relative and absolute terms. Thus, targeted unvaccinated testing programs lose effectiveness once vaccination rates exceed the threshold at which population immunity pushes R_{eff} below 1. These results echo related work focused on universal testing programs [8].

We estimate the vaccination rate that negates the impact of unvaccinated testing programs to be at most 92%, inclusive of social homophily and with a worst-case $R_0 = 6$, based on current estimates of the infection- and transmission-blocking effects of Pfizer and Moderna's mRNA vaccines [2]. However, baseline transmission rates are likely to be substantially lower due to changes in behavior such as social distancing and masking, compounded by the fact that naturally acquired immunity is estimated to provide similar infection- and transmission-blocking protections as mRNA vaccines [2]. As a consequence, actual vaccination rate thresholds, after which unvaccinated-only testing provides limited impact, are likely to be lower. On the other hand, if early reports of potential waning protection against COVID-19 disease [18] signal future decreases in VE_S and VE_I, required vaccination rates may be higher. The limited impact of testing programs focused on the unvaccinated population implies that once a community reaches a high vaccination rate, limited public health resources may be more effectively utilized elsewhere, including to further increase vaccination rates.

Our study predicts two other critical shifts as vaccination rates increase. First, when vaccination rates are sufficiently high, a majority of the albeit reduced number of infections will be vaccine breakthrough infections. This fact should come as no surprise, as this transition must occur at some point for any vaccine below 100% effectiveness; our modeling estimates it to take place between 75% and 81% vaccine coverage (Fig. 1, Supplementary Fig. S1). Second, while at low vaccination rates, community spread is driven by the unvaccinated population, at high vaccination rates (generally $\geq 85\%$), community spread is driven by vaccinated individuals or importation from neighboring communities. Taken together, these results suggest that while the overall number of cases in highly vaccinated communities will be low, vaccine breakthrough infections and transmission events from vaccinated individuals should not be surprising—vaccine effectiveness is not 100%. Consequently, in anticipation of continued community transmission even in highly vaccinated communities, those at increased risk of severe COVID-19 should take additional precautions to limit their risk of infection or severe disease.

Our analysis suggests that testing of the unvaccinated, when impactful, is most beneficial to the unvaccinated population. Nevertheless, testing focused on the unvaccinated population may provide additional incentives to get vaccinated and thus avoid regular testing. Our analyses strongly suggest that for such a testing program to be effective in reducing community transmission, testing must take place weekly or twice-weekly, and must have high rates of compliance; weekly testing with 50% compliance—a rate which reflects observed compliance in a population without major testing incentives [4]—is likely to be relatively

ineffective. However, it is important to note that while our analyses focus on the benefits of testing in reducing transmission, testing also plays an important role in diagnosis and treatment, detection of variants, situational awareness, and surveillance. Our study did not explore the benefits of unvaccinated-only testing regimens for these additional purposes.

Our analysis is limited in at least four different manners. First, our modeling incorporated fixed parameters that are difficult to estimate in practice. For instance, baseline SARS-CoV-2 transmission rates continue to shift with changes in policy and behavior, while VE_S and VE_I vary not only by vaccine manufacturer [2, 19] but may also decline over time [18]. Alternative parameter assumptions may be explored via the provided open-source code. Second, we assume perfect isolation after receiving a positive test result in all testing regimens, effectively removing all infectiousness once a diagnosis is received. Were this assumption to be violated by imperfect or delayed isolation, we predict a proportional loss of testing impact across all scenarios. Third, we have not explicitly modeled the impact of prior infection on either unvaccinated or vaccinated individuals. Due to the partial protection of prior infection against both infection and transmission [2], its inclusion would decrease the relative impact of testing focused solely on the unvaccinated, while also reducing the levels of vaccination required to achieve $R_{\text{eff}} = 1$. Nevertheless, in a community that is highly vaccinated, the marginal impact of prior infections may be relatively limited more broadly. Finally, we have assumed a relatively simple model by which homophily in contacts by vaccination status is implemented, such that populations are "well mixed" except for varying contact rates to reflect homophily. Richer spatially embedded or age-structured models may provide additional insights.

More broadly, our work is situated within a family of research which uses mathematical modeling to estimate the impact of targeted interventions or strategies in populations with heterogeneous susceptibility, transmissibility, and/or contact rates. Other areas of focus include the allocation of scarce personal protective equipment to reduce transmission [20], the prioritization of vaccines by subpopulation [21–23], proactive testing programs in specific workplace structures [24] or contact networks [8], immunity "passport" programs [17], or immune shielding strategies [25]. Our contribution to this literature is primarily to show that testing programs focused on the unvaccinated will substantially reduce transmission only if properly incentivized, and only until vaccination rates are sufficiently high as to obviate the need for this form of targeted intervention.

Acknowledgements

K.M.B. and C.E.M. were supported in part by the Interdisciplinary Quantitative Biology (IQ Biology) Ph.D. program at the BioFrontiers Institute, University of Colorado Boulder. C.E.M and D.B.L. were supported in part by the SeroNet program of the National Cancer Institute (1U01CA261277-01). R.P. was supported by the Howard Hughes Medical Institute.

Competing Interests Statement

R.P. is a founder of Faze Therapeutics. D.B.L. is an advisor to Darwin BioSciences and has received consulting fees from iCareDx. All other authors declare no conflicts of interest.

Data and Code Availability

All code is open source and provided by the authors at https://github.com/kbubar/unvacc_testing_in_mixed_pop_repo.

Materials and Methods

SEIR model

We used a continuous time ordinary differential equation compartmental model with Susceptible, Exposed, Infectious, and Recovered (SEIR) compartments, which were then stratified into vaccinated v and unvaccinated u groups. In addition to tracking infections among these two groups separately, we also tracked infections *from* both groups separately, enabling us to investigate four modes of transmission: from u to u, from u to v, from v to u, and from v to v. In all simulations, we used a constant total population size of $N = 20,000$ and let the vaccinated fraction of the population be parameterized by ϕ. We assumed that everyone in the vaccinated group was fully vaccinated at the start of each simulation, and that there was no ongoing vaccination. All simulations were run for 270 days, and all individuals were initially susceptible S_u or susceptible-vaccinated S_v. Model equations were solved using *lsoda* solver from the package deSolve, R version 4.1.0.

Vaccination was modeled to affect susceptibility to infection with effectiveness VE_S and transmissibility with effectiveness VE_I, placing our vaccine model in the broader category of leaky models [26]. Because our study focuses on transmission, we did not track disease, hospitalization, or mortality variables nor include vaccination's impacts on them. See Table S1 for parameter values for VE_S and VE_I used in the main text and sensitivity analyses.

To model a community with open boundaries, we included a uniform risk of exposure to infection from an external source at a rate of N^{-1} per person per day. For instance, in the absence of vaccination, S_u/N individuals would be infected per day. After including the protective effects of vaccination, this resulted in importation of infections at per-capita rates of N^{-1} and $(1 - \text{VE}_S)N^{-1}$ new infections per day in the susceptible-unvaccinated and susceptible-vaccinated groups respectively. Fig. S4 shows a model schematic diagram for the SEIR model used in the manuscript, where solid and dashed lines denote movement and transmission between classes, respectively.

Incorporation of testing

Testing, with subsequent isolation of those testing positive, was modeled by increasing the rate at which infected individuals were removed from the I_u compartment, and, because our modeling focuses on unvaccinated-only testing paradigms, these changes apply only to the unvaccinated population. We estimated increased rates of I_u removal using a previously established method that takes into account (i) the calibrated trajectories of viral loads within individual infection [27], (ii) the relationship between viral load and infectiousness [6], (iii) the frequency of testing, (iv) the test's analytical sensitivity (i.e. limit of detection) and turnaround time [17], and (v) testing compliance and valid sample rates, i.e. the fraction of scheduled or mandated tests which actually produce a valid sample [4]. In particular, our adaptation takes a previous model [6, 17] and updates viral load dynamics for the delta variant of SARS-CoV-2 [28, 29], the dominant variant at the time of the present analysis. To incorporate the effectiveness of testing θ, we reduce the duration of infectiousness $1/\gamma$ by a factor $(1 - \theta)$. Parameter values for θ are found in Table S1, and are based on PCR testing with a one-day turnaround, testing once or twice weekly, and compliance rates of 50% (as in [4]) or 99% (as in [7]). These values assume that individuals immediately and successfully isolate upon receiving a positive diagnosis. We note that estimated effects of rapid antigen tests (with higher analytical limits of detection, but zero turnaround time) are highly similar to PCR testing under the assumptions above, provided that testing program frequencies and compliance rates are identical [6].

To compute the total number of tests administered over the course of each simulation, we assumed the probability an unvaccinated individual was tested on any given day is $1/\delta$, where δ is the frequency of the testing regimen. We further assumed that unvaccinated individuals who previously received a positive test result were exempt from further testing requirements. Thus, the proportion of recovered individuals who continue to be tested are those who were not detected by testing during their infectious window i.e. $1 - \frac{1}{\delta\gamma}$, where γ is the recovery rate. Thus the total number of tests administered over the course of the simulation is

$$\sum_i \left(S_u(t_i) + E_u(t_i) + I_u(t_i) + \left(1 - \frac{1}{\delta\gamma}\right) R_u(t_i) \right) \frac{c}{\delta} \,,$$

where $c \in [0, 1]$ is the testing compliance, and t_i corresponds to day $i \in [0, 270]$.

Transmission modes and forces of infection

Inclusive of all effects introduced above, the forces of infection on the vaccinated and unvaccinated groups are

$$\begin{aligned} \lambda_v &= \left(\alpha \left[\frac{I_u}{N_u} c_{u\to v} + \frac{I_v}{N_v} c_{v\to v} (1 - \mathrm{VE}_I) \right] + \frac{1}{N} \right) (1 - \mathrm{VE}_S) \,, \\ \lambda_u &= \alpha \left[\frac{I_u}{N_u} c_{u\to u} + \frac{I_v}{N_v} c_{v\to u} (1 - \mathrm{VE}_I) \right] + \frac{1}{N} \,, \end{aligned} \tag{3}$$

where α is the probability of infection given a contact, tuned to achieve the desired R_0, $c_{i\to j}$ is the number of times an individual in group j is contacted by individuals from group i per day, and $N_v = \phi N$ and $N_u = (1 - \phi)N$ are convenience variables representing the total vaccinated and unvaccinated populations, respectively.

We calculated who is infecting whom at each time t by considering the different terms in $\lambda_v S_v(t)$ and $\lambda_u S_u(t)$ as follows:

Modes of transmission		Number of new infections at time t
unvaccinated	$\to$ unvaccinated	$\alpha \frac{I_u(t)}{N_u} c_{u\to u} S_u(t)$
	$\to$ vaccinated	$\alpha \frac{I_u(t)}{N_u} c_{u\to v} (1 - \mathrm{VE}_S) S_v(t)$
vaccinated	$\to$ unvaccinated	$\alpha \frac{I_v(t)}{N_v} c_{v\to u} (1 - \mathrm{VE}_I) S_u(t)$
	$\to$ vaccinated	$\alpha \frac{I_v(t)}{N_v} c_{v\to v} (1 - \mathrm{VE}_I)(1 - \mathrm{VE}_S) S_v(t)$
importation	$\to$ unvaccinated	S_u/N
	$\to$ vaccinated	$(1 - \mathrm{VE}_S) S_v/N$

To approximate how many cumulative infections one group caused in another group, we integrated each transmission mode over the duration of simulation, appromating the integral using the midpoint rule. For example, the cumulative number of unvaccinated infections caused by the unvaccinated is

$$\int_0^{270} \alpha \frac{I_u(t)}{N_u} c_{u\to u} S_u(t) dt \approx \frac{\alpha}{N_u} c_{u\to u} h \sum_{i=0}^{K} I_u(t_i) S_u(t_i),$$

where h is the timestep and $K - 1$ is the number of time intervals.

Reproductive number and homophily

This model's next generation matrix M, used to calculate the effective reproductive number R_{eff}, is given by

$$M = \alpha \begin{pmatrix} 1-\text{VE}_S & 0 \\ 0 & 1 \end{pmatrix} \begin{pmatrix} c_{v\to v} & c_{u\to v} \\ c_{v\to u} & c_{u\to u} \end{pmatrix} \begin{pmatrix} 1-\text{VE}_I & 0 \\ 0 & 1-\theta \end{pmatrix} \tag{4}$$

where C is the contact matrix for the vaccinated and unvaccinated groups. In a well-mixed population of $N\phi$ vaccinated and $N(1-\phi)$ unvaccinated individuals,

$$C_{\text{well mixed}} = N \begin{pmatrix} \phi & 1-\phi \\ \phi & 1-\phi \end{pmatrix} \tag{5}$$

This choice results in a reproductive number of

$$R_{\text{well mixed}} = R_0 \left[\phi(1-\text{VE}_S)(1-\text{VE}_I) + (1-\phi)(1-\theta)\right] \tag{6}$$

Homophily, the general tendency of people to associate with others who are similar to themselves, may affect the contact matrix C. Homophily in interactions based on vaccination status may be an active decision, where vaccinated individuals choose to primarily interact with others who are vaccinated, or a passive decision, where those who choose to be vaccinated are more likely to exist in a social network with others who choose to be vaccinated [30]. We included homophily in the contact matrix C by increasing within-group contacts and decreasing between-group contacts, subject to the constraint that homophily should not result in an overall increase or decrease in contacts—simply a rewiring of whom one contacts. We therefore adapted the "planted partition" model from network science [31, 32], which allows for adjustable levels of homophily while preserving overall contact rates between two equally sized groups, by applying it to unequal groups of sizes ϕN and $(1-\phi)N$. This modification required us to place an upper bound on the maximum within-group contact rates to avoid otherwise diverging contact rates when $\phi \to 0$ or $\phi \to 1$. Under these conditions, the contact matrix with homophily is

$$C_{\text{homophily}} = N \begin{pmatrix} \phi(2-\phi) & 1-\phi(2-\phi) \\ \frac{\phi^2[1-\phi(2-\phi)]}{(1-\phi)^2} & \frac{(1-\phi)^2-\phi^2[1-\phi(2-\phi)]}{(1-\phi)^2} \end{pmatrix}, \tag{7}$$

whose complete derivation may be found in Supplementary Text. The contact matrix for an adjustable level of homophily q is given by

$$C(q) = (1-q)\cdot C_{\text{well mixed}} + q \cdot C_{\text{homophily}}\ . \tag{8}$$

To compute the reproductive number of dynamics under homophily at level $0 \le q \le 1$, we substitute this contact matrix into Eq. (4) and compute the largest eigenvalue of the next generation matrix M. All plots and tables which include homophily use $q = 0.8$.

References

[1] Hana M. El Sahly, Lindsey R. Baden, Brandon Essink, Susanne Doblecki-Lewis, Judith M. Martin, Evan J. Anderson, Thomas B. Campbell, Jesse Clark, Lisa A. Jackson, Carl J. Fichtenbaum, Marcus Zervos, Bruce Rankin, Frank Eder, Gregory Feldman, Christina Kennelly, Laurie Han-Conrad, Michael Levin, Kathleen M. Neuzil, Lawrence Corey, Peter Gilbert, Holly Janes, Dean Follmann, Mary Marovich, Laura Polakowski, John R. Mascola, Julie E. Ledgerwood, Barney S. Graham, Allison August, Heather Clouting, Weiping Deng, Shu Han, Brett Leav, Deb Manzo, Rolando Pajon, Florian Schödel, Joanne E. Tomassini, Honghong Zhou, and Jacqueline Miller. Efficacy of the mRNA-1273 SARS-CoV-2 vaccine at completion of blinded phase. *New England Journal of Medicine*, Sep 2021.

[2] Toon Braeye, Laura Cornelissen, Lucy Catteau, Freek Haarhuis, Kristiaan Proesmans, Karin De Ridder, Achille Djiena, Romain Mahieu, Frances De Leeuw, Alex Dreuw, Naima Hammami, Sophie Quoilin, Herman Van Oyen, Chloé Wyndham-Thomas, and Dieter Van Cauteren. Vaccine effectiveness against infection and onwards transmission of COVID-19: Analysis of Belgian contact tracing data, January-June 2021. *Vaccine*, 39(39):5456–5460, Sep 2021.

[3] Anoop S.V. Shah, Ciara Gribben, Jennifer Bishop, Peter Hanlon, David Caldwell, Rachael Wood, Martin Reid, Jim McMenamin, David Goldberg, Diane Stockton, Sharon Hutchinson, Chris Robertson, Paul M. McKeigue, Helen M. Colhoun, and David A. McAllister. Effect of vaccination on transmission of SARS-CoV-2. *New England Journal of Medicine*, Sep 2021.

[4] Kristen K Bjorkman, Tassa K Saldi, Erika Lasda, Leisha Conners Bauer, Jennifer Kovarik, Patrick K Gonzales, Morgan R Fink, Kimngan L Tat, Cole R Hager, Jack C Davis, and et al. Higher viral load drives infrequent severe acute respiratory syndrome coronavirus 2 transmission between asymptomatic residence hall roommates. *The Journal of Infectious Diseases*, Jul 2021.

[5] Diana Rose E Ranoa, Robin L Holland, Fadi G Alnaji, Kelsie J Green, Leyi Wang, Richard L Fredrickson, Tong Wang, George N Wong, Johnny Uelmen, Sergei Maslov, et al. Mitigation of SARS-CoV-2 transmission at a large public university. *medRxiv*, 2021.

[6] Daniel B. Larremore, Bryan Wilder, Evan Lester, Soraya Shehata, James M. Burke, James A. Hay, Milind Tambe, Michael J. Mina, and Roy Parker. Test sensitivity is secondary to frequency and turnaround time for COVID-19 screening. *Science Advances*, 7(1), Jan 2021.

[7] Martin Pavelka, Kevin Van-Zandvoort, Sam Abbott, Katharine Sherratt, Marek Majdan, CMMID COVID-19 Working Group, Inštitút Zdravotnỳch Analỳz, Pavol Jarčuška, Marek Krajčí, Stefan Flasche, et al. The impact of population-wide rapid antigen testing on SARS-CoV-2 prevalence in Slovakia. *Science*, 372(6542):635–641, 2021.

[8] Ryan Seamus McGee, Julian R Homburger, Hannah E Williams, Carl T Bergstrom, and Alicia Y Zhou. Proactive COVID-19 testing in a partially vaccinated population. *medRxiv*, 2021.

[9] Biden mandates vaccines for workers, saying, 'Our patience is wearing thin'. *The New York Times*, Sept. 9, 2021. https://www.nytimes.com/2021/09/09/us/politics/biden-mandates-vaccines.html.

[10] Jason Horowitz. Italy puts in force tough new law requiring workers to test or vaccinate. *The New York Times*, Oct. 15, 2021. https://www.nytimes.com/2021/10/15/world/europe/italy-vaccination-law-covid.html.

[11] Centers for Disease Control and Prevention (CDC). Guidance for COVID-19 prevention in K-12 schools. https://www.cdc.gov/coronavirus/2019-ncov/community/schools-childcare/k-12-guidance.html, accessed Oct. 14, 2021.

[12] Centers for Disease Control and Prevention (CDC). COVID-19 Vaccinations in the United States. https://covid.cdc.gov/covid-data-tracker/#vaccinations_vacc-total-admin-rate-total, accessed Sept. 22, 2021.

[13] Mark EJ Woolhouse, C Dye, J-F Etard, T Smith, JD Charlwood, GP Garnett, P Hagan, JLK Hii, PD Ndhlovu, RJ Quinnell, et al. Heterogeneities in the transmission of infectious agents: implications for the design of control programs. *Proceedings of the National Academy of Sciences*, 94(1):338–342, 1997.

[14] Christopher Rose, Andrew J Medford, C Franklin Goldsmith, Tejs Vegge, Joshua S Weitz, and Andrew A Peterson. Heterogeneity in susceptibility dictates the order of epidemic models. *Journal of Theoretical Biology*, 528:110839, 2021.

[15] Hannah Ritchie, Edouard Mathieu, Lucas Rodés-Guirao, Cameron Appel, Charlie Giattino, Esteban Ortiz-Ospina, Joe Hasell, Bobbie Macdonald, Diana Beltekian, and Max Roser. Coronavirus pandemic (COVID-19). *Our World in Data*, 2021. https://ourworldindata.org/coronavirus.

[16] Amiel A. Dror, Netanel Eisenbach, Shahar Taiber, Nicole G. Morozov, Matti Mizrachi, Asaf Zigron, Samer Srouji, and Eyal Sela. Vaccine hesitancy: the next challenge in the fight against COVID-19. *European Journal of Epidemiology*, 35(8):775–779, Aug 2020.

[17] Daniel B. Larremore, Derek Toomre, and Roy Parker. Modeling the effectiveness of olfactory testing to limit SARS-CoV-2 transmission. *Nature Communications 2021 12:1*, 12(1):1–9, Jun 2021.

[18] Yair Goldberg, Micha Mandel, Yinon M Bar-On, Omri Bodenheimer, Laurence S Freedman, Eric Haas, Ron Milo, Sharon Alroy-Preis, Nachman Ash, and Amit Huppert. Waning immunity of the BNT162b2 vaccine: A nationwide study from Israel. *medRxiv*, 2021.

[19] Jamie Lopez Bernal, Nick Andrews, Charlotte Gower, Eileen Gallagher, Ruth Simmons, Simon Thelwall, Julia Stowe, Elise Tessier, Natalie Groves, Gavin Dabrera, et al. Effectiveness of COVID-19 vaccines against the B. 1.617. 2 (delta) variant. *New England Journal of Medicine*, pages 585–594, 2021.

[20] Colin J. Worby and Hsiao-Han Chang. Face mask use in the general population and optimal resource allocation during the COVID-19 pandemic. *Nature Communications*, 11(4049), 2020.

[21] Jan Medlock and Alison P Galvani. Optimizing influenza vaccine distribution. *Science*, 325(5948):1705–1708, 2009.

[22] Kate M Bubar, Kyle Reinholt, Stephen M Kissler, Marc Lipsitch, Sarah Cobey, Yonatan H Grad, and Daniel B Larremore. Model-informed COVID-19 vaccine prioritization strategies by age and serostatus. *Science*, 371(6532):916–921, 2021.

[23] Laura Matrajt, Julia Eaton, Tiffany Leung, and Elizabeth R Brown. Vaccine optimization for COVID-19: Who to vaccinate first? *Science Advances*, 7(6):eabf1374, 2021.

[24] Rowland W Pettit, Bo Peng, Patrick Yu, Peter Matos, Alexander L Greninger, Julie McCashin, and Christopher Ian Amos. Optimized post-vaccination strategies and preventative measures for SARS-CoV-2. *medRxiv*, 2021.

[25] Joshua S Weitz, Stephen J Beckett, Ashley R Coenen, David Demory, Marian Dominguez-Mirazo, Jonathan Dushoff, Chung-Yin Leung, Guanlin Li, Andreea Măgălie, Sang Woo Park, et al. Modeling shield immunity to reduce COVID-19 epidemic spread. *Nature medicine*, 26(6):849–854, 2020.

[26] M. Elizabeth Halloran, Michael Haber, and Jr. Longini, Ira M. Interpretation and estimation of vaccine efficacy under heterogeneity. *American Journal of Epidemiology*, 136(3):328–343.

[27] Muge Cevik, Matthew Tate, Ollie Lloyd, Alberto Enrico Maraolo, Jenna Schafers, and Antonia Ho. SARS-CoV-2, SARS-CoV, and MERS-CoV viral load dynamics, duration of viral shedding, and infectiousness: a systematic review and meta-analysis. *The Lancet Microbe*, 2(1):e13–e22, Jan 2021.

[28] François Blanquart, Clémence Abad, Joevin Ambroise, Mathieu Bernard, Gina Cosentino, Jean-Marc Giannoli, and Florence Débarre. Spread of the delta variant, vaccine effectiveness against PCR-detected infections and within-host viral load dynamics in the community in France. *HAL archives-ouvertes*, 2021.

[29] Stephen M. Kissler, Joseph R. Fauver, Christina Mack, Caroline G. Tai, Mallery I. Breban, Anne E. Watkins, Radhika M. Samant, Deverick J. Anderson, Jessica Metti, Gaurav Khullar, Rachel Baits, Matthew MacKay, Daisy Salgado, Tim Baker, Joel T. Dudley, Christopher E. Mason, David D. Ho, Nathan D. Grubaugh, and Yonatan H. Grad. Viral dynamics of SARS-CoV-2 variants in vaccinated and unvaccinated individuals. *medRxiv*, page 2021.02.16.21251535, Aug 2021.

[30] Pinelopi Konstantinou, Katerina Georgiou, Navin Kumar, Maria Kyprianidou, Christos Nicolaides, Maria Karekla, and Angelos P Kassianos. Transmission of vaccination attitudes and uptake based on social contagion theory: A scoping review. *Vaccines*, 9(6):607, 2021.

[31] Anne Condon and Richard M Karp. Algorithms for graph partitioning on the planted partition model. *Random Structures & Algorithms*, 18(2):116–140, 2001.

[32] Mark Newman. *Networks*. Oxford University Press, Oxford, United Kingdom, 2018. Second Edition, p 543.

[33] Nicholas Davies, Petra Klepac, Yang Liu, Kiesha Prem, Mark Jit, and Rosalind M Eggo. Age-dependent effects in the transmission and control of COVID-19 epidemics. *Nature Medicine*, 26(1205-1211), 2020.

[34] Bernard Cazelles, Benjamin Nguyen Van Yen, Clara Champagne, and Catherine Comiskey. Dynamics of the COVID-19 epidemic in Ireland under mitigation. *BMC Infectious Diseases*, 21(735), 2021.

Supplemental Figures and Tables

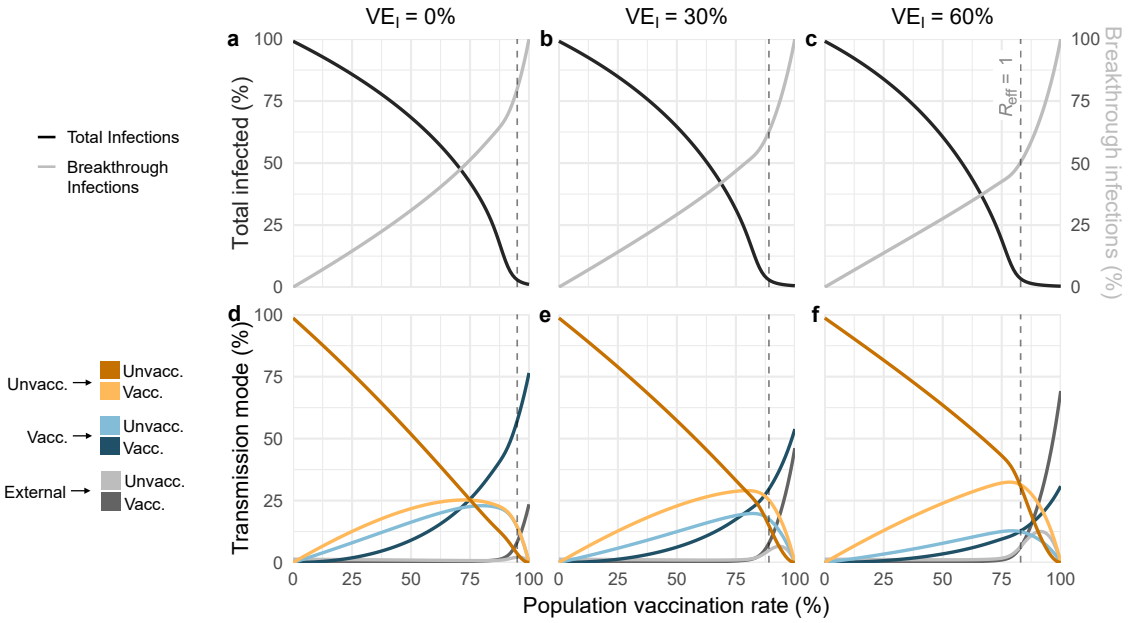

Figure S1: **Vaccination affects which populations drive transmission under various VE_I scenarios.** (a-c) Total infections over time (solid black), stratified by unvaccinated (dashed gray) and vaccinated (solid gray) populations, with a 55% vaccination rate. (d-f) Transmission mode as a percentage of total infections (see legend) for varying vaccination rates. Vertical dashed lines denote the vaccination rate at which $R_{\text{eff}} = 1$. (a,d) $VE_I = 0$, (b,e) $VE_I = 0.3$, (c,f) $VE_I = 0.6$. $R_0 = 4$ for all plots.

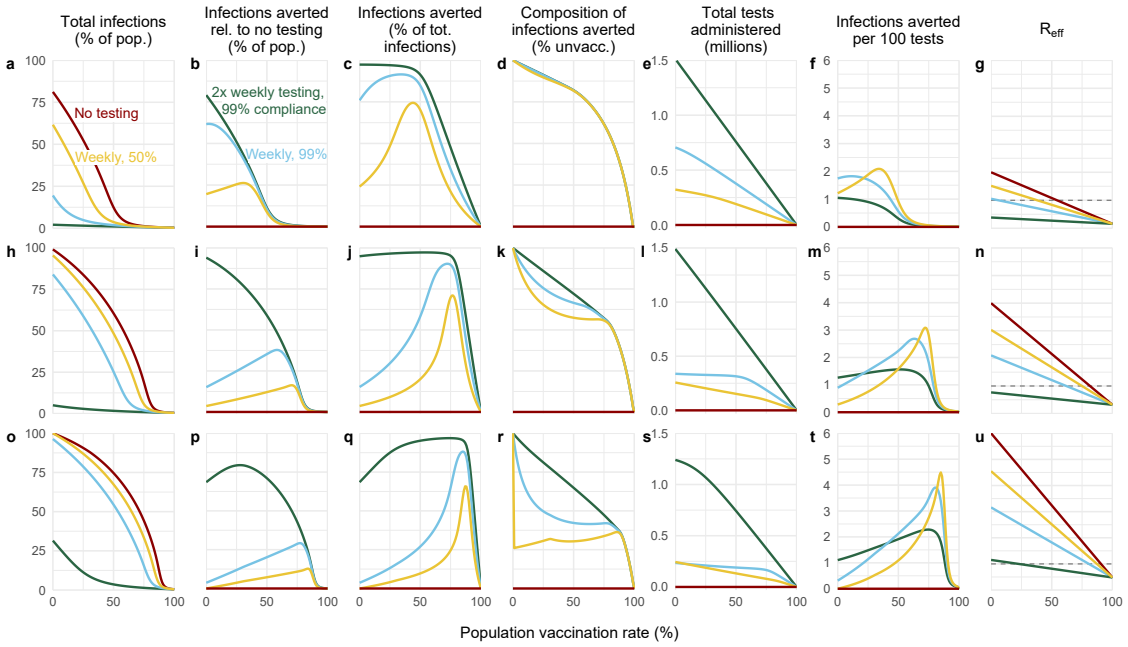

Figure S2: **Impact of unvaccinated-only testing on transmission.** Results are shown for varying vaccination rates under four testing regimens: no testing (red), weekly testing with 50% compliance (yellow), weekly testing with 99% compliance (blue), and twice-weekly testing with 99% compliance (green). (a,h,o) Percentage of population infected. (b,i,p) Percentage of potential infections averted due to testing. (c,j,q) Percentage of total infections averted due to testing. (d,k,r) percentage of total infections averted which were averted in the unvaccinated community. (e,l,s) Total number of tests administered (millions). (f,m,t) Infections averted per 100 tests. (g,n,u) Effective reproductive number R_{eff}. For all simulations, $\text{VE}_S = 0.80$ and $\text{VE}_I = 0.62$. Top row $R_0 = 2$. Middle row $R_0 = 4$. Bottom row $R_0 = 6$.

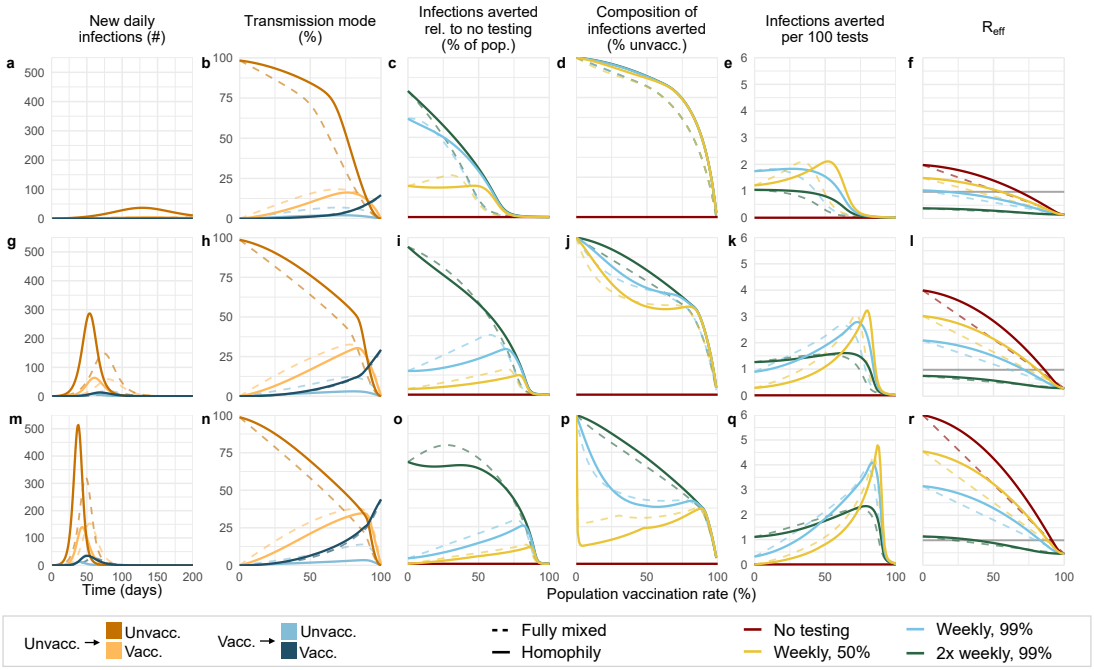

Figure S3: **Homophily affects transmission modes and impact of testing.** Panels contrast well-mixed contact patterns (no homophily; dashed lines) with homophilic contact patterns (solid lines) over multiple vaccination rates. (a) Homophily shifts the four modes of transmission, and in particular leads to increased $u \to u$. (b) Homophily increases $u \to u$ transmission across vaccination rates and (c) has mixed effects on the number of infections averted due to testing. (d) Homophily alters the composition of the infections averted by testing in both directions, as indicated by arrows. (e) Homophily shifts the number of infections averted per test lower. (f) Homophily increases the effective reproductive value (R_{eff}) non-linearly, except in instances where $R_{\text{eff}} < 1$ in the absence of homophily. Top row $R_0 = 2$. Middle row $R_0 = 4$. Bottom row $R_0 = 6$.

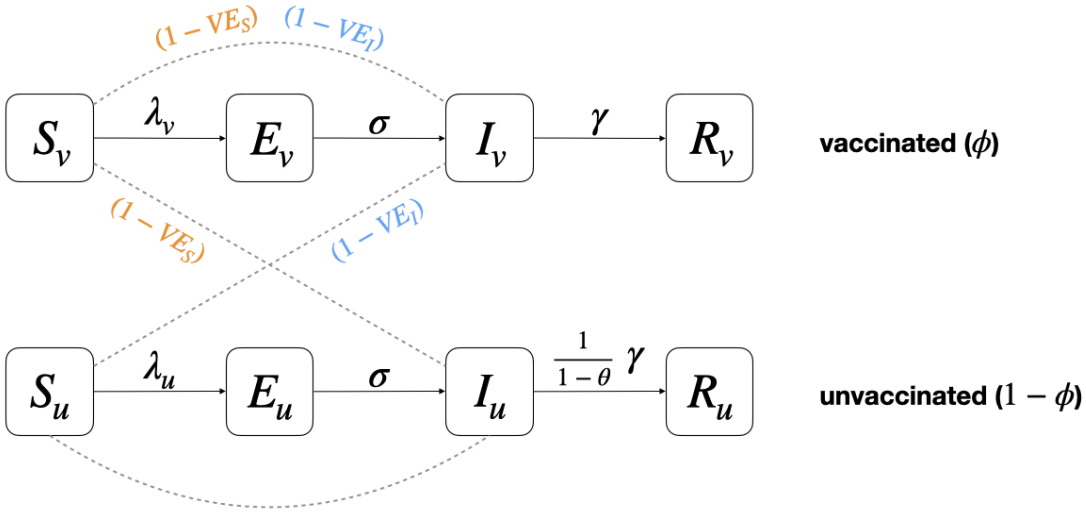

Figure S4: **SEIR Model Flow Diagram.** SEIR model schematic depicting unvaccinated (u subscript) and vaccinated (v subscript). Solid lines denote movement of individuals between classes at the given rate. The time spent infectious, $1/\gamma$, may be shortened by a factor of $1-\theta$ due to testing. Dashed lines denote infectious interactions, scaled by vaccine protection against infection (VE_S) and transmission (VE_I).

Parameter	Description	Value	Reference
Infection parameters			
σ^{-1}	Latent period	3 days	[33]
γ^{-1}	Infectious period	6 days	[34]
R_0	Basic reproductive number	$\{2, 4, 6\}$	—
α	Probability of transmission given contact (tuned to achieve the desired R_0)	$R_0\gamma/N$	—
Vaccine parameters			
ϕ	Proportion of population vaccinated	$[0, 1]$ US: 0.55	[12]
VE_S	Vaccine effectiveness to decrease susceptibility	80%	[2]
VE_I	Vaccine effectiveness to decrease infectiousness	62%	[2]
Population parameters			
N	Population size	20,000	—
q	Homophily parameter	0.8	see Methods
Testing parameters			
θ	Fraction by which testing & isolation reduces typical *unvaccinated* infectious period*		
	no testing	0	—
	weekly testing, 50% compliance	0.242	[6]
	weekly testing, 99% compliance	0.473	[6]
	2× weekly testing, 99% compliance	0.808	[6]

Table S1: **Summary of parameters used in modeling and simulation.**
*Assuming PCR testing with a one day turnaround time for test results.

Proportion of population vaccinated (%) when cumulative transmission is no longer dominated by unvaccinated							
		well mixed			homophily		
R_0		2	4	6	2	4	6
Testing	no testing	74	86	80	81	89	84
	weekly testing, 50% compliance	66	82	77	75	86	82
	weekly testing, 99% compliance	51	74	72	64	80	79
	2× weekly, 99% compliance	0	33	53	0	47	63

Table S2: **Vaccination rate at which the dominant mode of transmission shifts under moderate VE_I assumption.** R_0 values of 2, 4, and 6 are considered under well mixed ($q = 0$) and homphilic ($q = 0.8$) mixing assumptions. $\text{VE}_S = 80\%, \text{VE}_I = 30\%$.

Proportion of population vaccinated (%) when cumulative transmission is no longer dominated by unvaccinated							
		well mixed			homophily		
R_0		2	4	6	2	4	6
Testing	no testing	74	76	71	80	83	75
	weekly testing, 50% compliance	65	72	67	75	80	72
	weekly, 99% compliance	51	67	61	63	77	67
	2× weekly, 99% compliance	0	32	43	0	46	52

Table S3: **Vaccination rate at which the dominant mode of transmission shifts under low VE_I assumption.** R_0 values of 2, 4, and 6 are considered under well mixed ($q = 0$) and homphilic ($q = 0.8$) mixing assumptions. $\text{VE}_S = 80\%, \text{VE}_I = 0\%$.

Supplementary Text: Derivation of Contact Matrix with Homophily

In Materials and Methods, we state a contact matrix with homophily but omit its complete derivation. The purpose of this Supplementary Text is to explain the derivation in full detail, and to motivate the need for such a complicated looking matrix.

In network science, the planted partition model is a convenient model for contact structure with homophily [31]. In it, one imagines a well-mixed population with two groups, such that a u's propensity to contact other us is equal to their propensity to contact vs. If there are ϕN people in group u and $(1-\phi)N$ in group v, then an individual in either group will have contact rates with the two groups proportional to ϕN and $(1-\phi)N$, respectively. This is what is shown in the definition of $C_{\text{well mixed}}$ in Materials and Methods.

To achieve homophily, the planted partition model then imagines that a fraction q of between-group connections are "rewired" to be within-group connections. This would result in a contact matrix of

$$C_{\text{planted partition}} = N \begin{pmatrix} \phi + q(1-\phi) & (1-q)(1-\phi) \\ (1-q)\phi & 1-\phi+q\phi \end{pmatrix} , \tag{S1}$$

where $q = 0$ recovers the well-mixed matrix. Unfortunately, this model results in nonsensical contact patterns for $\phi \to 0$ or $\phi \to 1$, with the rewired contacts becoming concentrated in a smaller and smaller group. Contact rates reach nonsensical levels, and this simplified model of homophily, while mathematically convenient, fails to capture anything close to realistic contact rates. We note that this problem does not surface in the network science literature because, typically, two equal-sized communities are considered, and therefore $\phi = 0.5$ so contact rates are well bounded.

To address this issue, we consider a similar model for homophily, but with an upper bound on how much the within-group contact rate may increase. Let $r(\phi)$ be the maximum factor by which $v \to v$ contact rates may increase. In order for the total contact rates to balance, it must be the case that

$$\phi \cdot r(\phi) + (1-\phi) \cdot x_{u\to v} = 1 , \tag{S2}$$

where $x_{u\to v}$ is the factor governing how vs are contacted by us. Thus,

$$x_{u\to v} = \frac{1-\phi \cdot r(\phi)}{1-\phi} . \tag{S3}$$

Any adjustment to the rate at which each v is contacted by u must be balanced by the rate at which each u is contacted by each v, which means that

$$x_{v\to u} = \frac{\phi}{1-\phi} \cdot x_{u\to v} = \phi \frac{1-\phi \cdot r(\phi)}{(1-\phi)^2} . \tag{S4}$$

Finally, repeating the argument of Eq. (S2) but for u, we get

$$\phi \cdot x_{v\to u} + (1-\phi) \cdot x_{u\to u} = 1 ,$$

implying that

$$x_{u\to u} = \frac{1-\phi \cdot x_{v\to u}}{1-\phi} = \frac{(1-\phi)^2 - \phi^2(1-\phi \cdot r(\phi))}{(1-\phi)^3} . \tag{S5}$$

In summary, the matrix of factors by which contacts will be adjusted for homophily is

$$X = \begin{pmatrix} r(\phi) & \frac{1-\phi\cdot r(\phi)}{1-\phi} \\ \phi\frac{1-\phi\cdot r(\phi)}{(1-\phi)^2} & \frac{(1-\phi)^2-\phi^2(1-\phi\cdot r(\phi))}{(1-\phi)^3} \end{pmatrix} , \tag{S6}$$

a matrix with the interesting property that it is fully specified after $r(\phi)$ is specified. Critically, it also ensures that the total contact rate experienced by each individual is unaltered, regardless of the choice of the factor $r(\phi)$.

Two additional constraints allow us to specify $r(\phi)$ exactly. The first constraint is that homophily should have the same effects on the vaccinated and unvaccinated populations, meaning that our model should not, for instance, simply increase $v \to v$ contact rates without also increasing $u \to u$ rates. Mathematically, we express this constraint as

$$x_{u\to u}(1-\phi) = x_{v\to v}(\phi) .$$

The second constraint is that the rewiring effect should not increase the connection factors without bound too much as the smaller group shrinks,

$$\lim_{\phi\to 0} [x_{v\to v}(\phi) + x_{u\to u}(\phi)] = M \ll N .$$

Enforcing these two constraints at once, we get

$$r(\phi) + \frac{(1-\phi)^2 - \phi^2(1-\phi\cdot r(\phi))}{(1-\phi)^3} = M \tag{S7}$$

and solving for $r(\phi)$ produces the rational function

$$r(\phi) = \frac{M(1-\phi)^3 + \phi^2 - (1-\phi)^2}{\phi^3 + (1-\phi)^3} . \tag{S8}$$

In this manuscript, we let $M = 3$, which yields the surprisingly simple $r(\phi) = 2 - \phi$. Alternative larger choices of the bound M are naturally also possible, though higher values lead to increasingly unrealistic maximum within-group contact rates.

To convert the matrix of homophily factors X into actual contact rates, we multiply X element-wise by the well-mixed contact rates it is designed to enhance, producing

$$\begin{aligned} C_{\text{homophily}} &= N \begin{pmatrix} \phi\cdot r(\phi) & (1-\phi)\cdot\frac{1-\phi\cdot r(\phi)}{1-\phi} \\ \phi\cdot\phi\frac{1-\phi\cdot r(\phi)}{(1-\phi)^2} & (1-\phi)\cdot\frac{(1-\phi)^2-\phi^2(1-\phi\cdot r(\phi))}{(1-\phi)^3} \end{pmatrix} \\ &= N \begin{pmatrix} \phi r(\phi) & 1-\phi r(\phi) \\ \phi^2\frac{1-\phi r(\phi)}{(1-\phi)^2} & \frac{(1-\phi)^2-\phi^2(1-\phi r(\phi))}{(1-\phi)^2} \end{pmatrix} . \end{aligned} \tag{S9}$$

Finally, we let the actual contact rates be a mixture of $C_{\text{well mixed}}$ and $C_{\text{homophily}}$, parameterized by q, such that $q = 0$ yields well-mixed contacts and $q = 1$ yields maximally homophilic contacts,

$$C(q) = (1-q)\cdot C_{\text{well mixed}} + q\cdot C_{\text{homophily}} . \tag{S10}$$

Choosing $M = 3$ (and thus $r(\phi) = 2 - \phi$) yields the equation in Materials and Methods.